LUT University

Shell-and-tube heat exchanger optimization - impact of problem formulation and cost function

Saari Jussi, Garcia Perez Manuel, Vianna Neto Marcio, Cardoso Marcelo, Vakkilainen Esa, Kaikko Juha

This is a Publisher's version version of a publication

published by HEFAT

in The 14th International Conference on Heat Transfer, Fluid Mechanics and Thermodynamics HEFAT2019

DOI:

Copyright of the original publication: © Jussi Saari 2019

Please cite the publication as follows:

Saari J., García Perez M., Vianna Neto M., Cardoso M., Vakkilainen E., Kaikko J. (2019). Proceedings of the 14th International Conference on Heat Transfer, Fluid Mechanics and Thermodynamics in Wicklow, Ireland, 22nd-24th July 2019, pp.1350-1356.

This is a parallel published version of an original publication. This version can differ from the original published article.

SHELL-AND-TUBE HEAT EXCHANGER OPTIMIZATION - IMPACT OF PROBLEM FORMULATION AND COST FUNCTION

Saari J.*[a] , García Pérez M [b], Vianna Neto M.[c], Cardoso M.[c], Vakkilainen E.[a], and Kaikko J.[a].
*Author for correspondence
a Lappeenranta University of Technology, P.O.Box 20, FI-53851 Lappeenranta, Finland
E-mail: saari@lut.fi
b CERN, Route de Meyrin, 1211 Genève, Switzerland
c Universidade Federal de Minas Gerais, Av. Antônio Carlos 6627, CEP: 31270-901, Belo Horizonte, Brazil

ABSTRACT

The design optimization of shell-and-tube heat exchangers (STHEs) is studied. Impact of using standard lengths and shell diameters is investigated, and two types of cost function are compared: a simple area-based correlation typically used in STHE optimization studies, and a more detailed one. Special emphasis is placed on selecting the decision variables. The most difficult problem, the discrete one, is evaluated with four decision variable choices. Both the problem formulation and cost function proved important for the convergence rate as well as the solutions found. The simple area-based cost correlation was confirmed to be severely limited for optimization purposes.

INTRODUCTION

Shell-and-tube heat exchangers (STHEs) can be designed to operate with a wide range of pressures, temperatures, and fluids. Due to this flexibility, they are the most common heat exchanger type in many industries. Most common is the segmentally baffled STHE with one shell pass an even number of tube passes.

STHE design optimization has been studied and published extensively, using a variety of methods used for heat transfer, pressure drop and cost modeling, as well as the optimization itself. Total annual cost including capital and energy costs has been a common objective function [1-7], but also other objectives such as equipment cost minimization [9-11], effectiveness maximization [12], and entropy minimization [13] have been used. Multi-objective optimization examples include heat transfer maximization while minimizing cost [14] or pressure drop [15], minimizing pumping cost and area [16], and maximizing effectiveness while minimizing cost [17].

STHE optimization is in many ways a difficult problem. Typical construction and design options with several discrete, non-continuous variables makes the cost function ill-behaved: multi-constrained, non-differentiable and often multimodal. These issues have been addressed in a number of ways, each with some drawbacks. Early examples include a deterministic, non-iterative solution combining pumping and area costs presented by Jegede and Polley [5] and improved by Serna and Jiménez [18], general disjunctive programming [6], graphical analysis [7], and systematic tube count table screening with heuristic pruning [11]. To reduce the risk of finding only a local optimum, stochastic global optimization methods have been used. The drawback of these is the long computational times, but as CPU speeds increase, this becomes less of a problem in contrast to the robustness and easy implementation. Stochastic methods applied to STHE optimization include simulated annealing [10], particle swarm [4,18], and various evolutionary algorithms such as differential evolution (DE) [9], genetic algorithms (GA) [3,4,12-15], and harmony search [20].

As new metaheuristics are developed, they are applied on STHE optimization. Solutions using new methods are often compared to those found in earlier studies, but little attention has been paid to the impact of other factors than the choice of optimizer. While not affecting the optimal design or objective function value, the choice of decision variables versus those calculated as functions thereof does change the objective function topography, potentially compromising comparisons.

An important factor in problem formulation is also the cost function. Most STHE optimization studies have estimated costs by simple area-based correlations. This reduces computation time, but such functions may yield unrealistic results. While this drawback has been pointed out [21], a careful evaluation of the impact of the cost function on the optimized configuration has not yet been performed. This study investigates whether simple correlations can be useful for finding the optimal configurations, and if not, could they still be useful as surrogates for more detailed cost models for optimizer performance evaluation. Genetic algorithm, a well-known metaheuristic based on natural evolution was used. Two different cost functions, and both discrete and continuous problem formulations are compared.

NOMENCLATURE

A	[m^2]	Area
BC	[-]	Baffle cut fraction
c_{el}	[€/kWh]	Cost of electricity
C_f	[-]	Coefficient of friction (Fanning)
C_{FOB}	[€,USD]	Cost, Free On Board
C_{inv}	[€,USD]	Cost, investment
C_{man}	[€,USD]	Cost, total manufacturing
C_{mat}	[€,USD]	Cost, materials
C_{pr}	[€,USD]	Cost, manufacturing processes
C_{tot}	[€,USD]	Total annual cost (operation + investment amortization)
CF	[-]	Crossover fraction in genetic algorithm
d	[m]	Tube diameter
D	[m],[-]	1. diameter
		2. number of decision variables in optimization problem
f	[-]	Friction factor (Darcy)
FA	[-]	Fluid assignment binary variable
G	[-]	Generation in genetic algorithm
h	[W/m^{2}K]	Heat transfer coefficient
i	[-]	Interest rate
k	[W/mK]	Thermal conductivity
K	[-]	1. parameter for bundle diameter – tube count correlation
		2. loss coefficient
		3. absolute surface roughness
L	[m]	Length
$\dot{m}$	[kg/s]	Mass flow rate

MS	[-]	Mutation scale parameter in genetic algorithm
n	[a],[-]	1. investment amortization time 2. parameter for bundle diameter – tube count correlation
N_{bfl}	[-]	Number of baffle plates
N_E	[-]	Elite count parameter in genetic algorithm
N_{ss}	[-]	Number of sealing strips
N_{tb}	[-]	Number of tubes
N_{tp}	[-]	Number of tube passes
NFE	[-]	Number of function evaluations
NP	[-]	Number of parents (population size)
NTU	[-]	Number of transfer units
Nu	[-]	Nusselt number
P	[m]	Tube pitch
Pr	[-]	Prandtl number
R	[m^{2}K/W]	Thermal resistance
S	[-]	Shrink parameter in genetic algorithm
S_{bfl}	[m]	Baffle distance
T	[°C]	Temperature
t	[s]	Time
U	[W/m^{2}K]	Overall heat transfer coefficient
w	[m/s]	Velocity

Special characters

Δp	[Pa]	Pressure drop
ε	[-]	Heat exchanger effectiveness
Φ	[W]	Heat transfer rate
η_m	[-]	Electric motor efficiency
η_p	[-]	Pump efficiency
μ	[Pa s]	Dynamic viscosity
ρ	[kg/m^3]	Density
θ_{tp}	[°]	Tube layout staggering angle
ψ	[-]	Shell-side void fraction

Subscripts

c	Cold fluid
C	Equipment cost based on method by Caputo et al.
h	Hot fluid
H	Equipment cost according to correlation by Hall et al.
i	Tube inside
in	Inlet
nzl	Nozzle
o	Tube outside
out	Outlet
OTL	Outer Tube Limit
sh	Shell
tb	Tube
tot	Maximum dimensions of entire heat exchanger
wi	Tube-side fluid, wall conditions

OPTIMIZATION PROBLEMS CONSIDERED

Objective Functions

Minimizing the total annual cost C_{tot} consisting of equipment and operating costs is considered, using three problem formulations: A, B and C. Formulation A uses a common area-based cost correlation, while problems B and C implement a more detailed cost model to prevent the free use of features that increase the cost without affecting area. Objective functions can differ also in how the STHE is defined, i.e. which are the decision variables, and which are solved from those. Standard dimensions, or an even number of passes for piping simplicity may be preferred; the same case can have very different objective function topologies depending on problem formulation. Here the problem formulations A and B use continuous variables describing the flows as decision variables when possible, while in problem C decision variables are mainly equipment dimensions chosen from a discrete set of standard dimensions.

The operating cost is the product of pump power use and electricity price. The time value of money is considered by dividing the C_{inv} to equal amortizations over n years, yielding

$$C_{tot} = \frac{i(1+i)^n}{(1+i)^n-1} C_{inv} + \left[\frac{\left(\frac{\dot{m}_c}{\rho_c}\right)\Delta p_c}{\eta_p \eta_m} + \frac{\left(\frac{\dot{m}_h}{\rho_h}\right)\Delta p_h}{\eta_p \eta_m}\right] t\, c_{el} \qquad (1)$$

where C_{inv} is the capital investment. An interest rate i = 10%, payback time n = 10 a, annual operating time t = 7000 h and an electricity cost of c_{el} = 120 €/MWh are considered; pump and electric motor efficiencies are η_p = 0.70 and η_m = 0.85. For estimating the investment cost C_{inv}, the heat transfer surface sizing was first performed using the ε-NTU method and the STHE heat transfer model (see Appendix A).

In problem A the C_{inv} [USD] is calculated from heat transfer area A by the often-used correlation based on cost data from Hall et al. [22] as referred in [21] for stainless steel construction:

$$C_{inv} = 8000 + 259.2\, A^{0.91} \qquad (2)$$

In problems B and C the investment cost C_{inv} [€] for installed STHE is estimated as 3.3 times the FOB cost C_{FOB}[23], which is found from manufacturing cost C_{man} using a mark-up estimate based on 30% overhead cost, 5% contingency and 10% profit for manufacturer (reference cost data in €). The manufacturing cost is the sum of material cost C_{mat} and manufacturing process cost C_{pr}. These are determined by a cost model based on that of [24], which itself is a simplified implementation of the one in [21]. The model considers the material costs of the main parts: shell, tubes, tubesheet, baffles, front and rear head channels, flanges, and possible shell-side sealing strips. The sizing of these is performed with the methodology developed and described in [25]. The manufacturing process cost C_{pr} is the sum of costs of tube hole drilling and bevelling, sheet cutting for baffle and sealing strips, and tube bundle assembly. The cost of tubes is estimated as a function of tube diameter based on commercial data as in reference [24].

The problem formulations for the cases are summarized in Table 1. Discrete variables are marked with an asterisk.

Table 1 STHE optimization problems considered

	Problem A	**Problem B**	**Problem C**
Cost function:	$f(A)$, Eq.(2)	$C_{mat}+C_{pr}$	$C_{mat}+C_{pr}$
$\boldsymbol{x_1}$	θ_{tp} [°] *	θ_{tp} [°] *	θ_{tp} [°] *
$\boldsymbol{x_2}$	N_{tp} [-] *	N_{tp} [-] *	N_{tp} [-] *
$\boldsymbol{x_3}$	FA [-] *	FA [-] *	FA [-] *
$\boldsymbol{x_4}$	d_o [mm] *	d_o [mm] *	d_o [mm] *
$\boldsymbol{x_5}$	P/d_o [-]	P/d_o [-]	$N_{tb/p}$ [-] *
$\boldsymbol{x_6}$	S_{bf}/D_{sh} [-]	S_{bf}/D_{sh} [-]	L_{tb} [m] *
$\boldsymbol{x_7}$	N_{SS} [-] *	N_{SS} [-] *	N_{SS} [-] *
$\boldsymbol{x_8}$	w_{tb} [m/s]	w_{tb} [m/s]	N_{bf} [-] *
$\boldsymbol{x_9}$	BC [-]	BC [-]	BC [-]
$\boldsymbol{x_{10}}$			D_{sh} [m] *

* discrete variable

In problems A and B the tube-side velocity and pitch ratio P/d_o are known. From these the tube count N_{tb} and diameter of tube bundle (D_{OTL}) and shell (D_{sh}) are calculated. In case C, the N_{tb} and D_{sh} are known and the tube pitch ratio is calculated. The

relationship between N_{tb} and D_{OTL} are shown in equation (3), using the constants of Table 2.[23]

$$N_{tb} = \left(\frac{1.25 d_o}{P}\right)^2 \cdot K_1 \left(\frac{D_{OTL}}{d_o}\right)^{n_1} \quad (3)$$

The variables and their ranges are listed in Table 3; Figure 1 shows the staggering angle θ_{tp}. Binary variable FA=0 means the cold fluid is in the tubes and hot at the shell side; 1 the opposite.

Table 2 Constants used in equation (3).

	θ_{tp} = 30°, 60°		θ_{tp} = 45°, 90°	
N_{tp}	K_1	n_1	K_1	n_1
1	0.319	2.142	0.215	2.207
2	0.249	2.207	0.156	2.291
4	0.175	2.285	0.158	2.263
6	0.0743	2.499	0.0402	2.617
8	0.0365	2.675	0.0331	2.643

Table 3. Decision variables and their acceptable ranges

Variable	Range
Tube layout θ_{tp} [°]	{30, 45, 60}
Tube passes N_{tp} [-]	{1, 2, 4, 6, 8}
Fluid assignment FA [-]	{0, 1}
Tube outside diameter d_o [mm]	{9.52, 12.70, 15.88, 19.05, 22.2, 25.4, 31.8, 38.1, 50.8}
Tube pitch ratio P/d_o [-]	$1.25 \le P/d_o \le 2$
Tubes per pass $N_{tb/p}$ [-]**	$20 \le N_{tb/p} \le 1200$
Baffle/shell ratio S_{bf}/D_{sh}[-]*	$0.20 \le S_{bf}/D_{sh} \le 1$
Sealing strip pairs N_{SS} [-]	{0,1,…,7}
Velocity (tube) w_{tb} [m/s]*	$0.4 < w_{tb} < 2.5$
Baffle cut BC [-]	$0.15 < BC < 0.4$
Tube length L_{tb} [m]**	{1.219, 1.829, 2.438, 3.048, 3.658, 4.877, 6.096, 7.315}
Number of baffles N_{bf} [-]**	{3, 4, …, 25}
Shell diameter D_{sh} [m]**	{0.203, 0.254, 0.305, 0.337, 0.387, 0.438, 0.489, 0.540, 0.591, 0.635, 0.686, 0.737, 0.787, 0.838, 0.889, 0.940, 0.991, 1.067, 1.143, 1.219, 1.295, 1.372, 1.448, 1.524}

* only cases A and B
** only case C

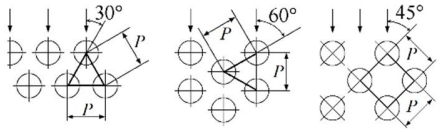

Figure 1 Tube staggering angles θ_{tp}.

Studied Application Cases

Two application cases often used in STHE optimization studies are considered. Case 1 represents the example from [23] where methanol is cooled with brackish water, while Case 2 is a heat exchanger from an oil refinery crude preheat train with kerosene heating the crude oil. Both are summarized in Table 4.

Table 4. Fluids and heat transfer rates of considered cases.

Case, Φ	Fluid	$\dot{m}$ [kg/s]	T_i / T_o [°C]	R''_{tf} [m²K/W]
Case 1, 4.34 MW	Methanol	27.78	95.0 / 40.0	$3.3 \cdot 10^{-4}$
	Brackish water	68.88	25.0 / 40.0	$2.0 \cdot 10^{-4}$
Case 2, 1.44 MW	Kerosene	5.52	199 / 93.3	$6.1 \cdot 10^{-4}$
	Crude Oil	18.80	37.8 / 76.7	$6.1 \cdot 10^{-4}$

Several constraints due to to manufacturing, transportation, and mechanical cleaning of the heat transfer surfaces limit the design choices. These are listed in Table 5. Case 2, where both fluids are severely fouling and both sides may need mechanical cleaning, has additional geometry requirements: square tube layout, 6.5 mm minimum gap between the tubes, 19.05 mm minimum tube diameter, and a pull-through floating head design (TEMA AET) to provide access to both tube and shell side. Case 1 fluids are relatively clean (methanol) and moderately fouling (water), and TEMA AEL is used in case of 1-pass construction to provide tubesheet cleaning access without dismantling piping. If an even number of tube passes is used, TEMA AEM with bonnet rear head is sufficient to provide access in Case 1.

Table 5. Constraints.

Variable	1A	1B	1C	2A	2B	2C
θ_{tp} [°]				45	45	45
N_{tp} [-]				even	even	even
Tube fluid				cold	cold	cold
d_o [mm]					≥ 19.05	≥ 19.05
P-d_o [mm]	≥ 3.2	≥ 3.2	≥ 3.2	≥ 6.5	≥ 6.5	≥ 6.5
D_{tot} [m]	< 3.5	< 3.5	< 3.5	< 3.5	< 3.5	< 3.5
L_{tot} [m]	< 15.0	< 15.0	< 15.0	< 15.0	< 15.0	< 15.0

Fouling has both thermal and pressure drop (Δp) effects. The thermal resistance R''_{tf} accounts for the net sum of all heat transfer effects: conduction resistance, surface roughness change and flow velocity change. In most STHE optimization studies the Δp effect is neglected; this was done with problem A here. Significant fouling can make Δp effects relevant, however; this is considered in problem formulations B and C. The foulant thickness is estimated assuming conduction resistance defined by the foulant conductivity k_f to dominate the heat transfer effect. Brackish water fouling is considered biofouling, with k_f = 0.7 W/mK.[26] Crude oil foulants start at ~0.2 W/mK but turn to coke (1 W/mK) with time and also contain minerals with higher k_f [27]; here 0.5 W/mK is assumed. For kerosene and methanol conductivities of the fluids are used in the absence of better data. The foulant thicknesses are added to d_o and deducted from d_i to obtain the fouled diameters and the resulting flow velocities.

Genetic Algorithm

The GA supplied with MATLAB Global Optimization toolbox is used.[28] As an evolutionary algorithm it operates with populations of trial solutions. New solutions are produced in each iteration by crossover and mutation. Members of the last complete generation G are referred to as the parents, those of G+1 as the offspring. Elitism is applied to ensure the best solutions are not lost: a number of best solutions, set by the elite count parameter N_E, survive unchanged to generation G+1.

The crossover fraction CF sets the fraction of offspring created by crossover. In the so-called scattered crossover implemented here, two candidate solutions of generation G are chosen to serve as parents, and variable values are taken randomly from one or the other to create the child. The remainder of G+1 is created by mutation. A mutant is generated from a parent by summing to it a vector of Gaussian-distributed random variables with a mean of zero and a reducing standard deviation. The initial standard deviation for the mutation of variable d of the first generation G=1 is set based on mutation scale parameter MS and the allowed range of decision variable d as

$$\sigma_1^{\mathrm{d}} = MS \cdot \left(x_{\mathrm{d,max}} - x_{\mathrm{d,min}}\right) \quad (4)$$

For each following generation G, the corresponding standard deviation σ_G is obtained using a shrink parameter S and the maximum number of generations G_{max} so that as the evolution proceeds, the mutation scale reduces:

$$\sigma_G = \sigma_{G-1}\left(1 - S\frac{G}{G_{\max}}\right). \quad (5)$$

Selection pressure is applied at parent selection: the better the objective function value of an solution, the better it's chance to become a parent for mutation or crossover.

RESULTS AND DISCUSSION

The first step was to find the best solutions for each case. While there is no proof of global convergence in finite time for any of the tested algorithms, it was considered likely that of several long runs at conservative tuning parameter values, some would likely find the optimum. The GA was ran five times for each case at NP=200D until reaching 10^6 function evaluations.

The total costs of formulations A were clearly less than the others. This is due to equipment cost equation (2) being used as presented by Hall et al. in 1982 without a cost index correction. It is used in this form for comparability of results, as the majority of recent STHE optimization publications have not used index corrections. Combined with modern-day electricity prices, the optimization then also yields much lower Δp than in problem formulations B and C, but similar to the results of many other studies, e.g. [8], [29-31]. The cost could be corrected by an index to current level, but being based only on tube area causes also other serious deficiencies, evident in Table 6. If the material and manufacturing costs of other components such as sealing strips are neglected, their effect is reduced to heat transfer and pressure drop alone. In case of the sealing strips this puts the optima at the maximum allowed, but assigning for strips the same material cost as for baffles and considering plate cutting, optimum becomes zero (Case 1), or with the larger bundle-to-shell gap of floating-head designs, 1 to 2 pairs (Case 2). Cases 1A and 2A use USD instead of EUR to facilitate comparison with earlier studies; results are thus not comparable to formulations B and C, but optimization performance comparison is unaffected.

The tube size, count and pitch are broadly similar among all sub-cases of 1. With Case 2, the arrangement becomes unusual if sub-case A used: very small 9.52 mm tubes placed sparsely in the shell (P/d_o = 1.85). While clearly unrealistic, this is similar to the small 12.7 mm tubes found in [8] with GA and in [9] by DE. The reasons for this are both neglecting costs other than the heat transfer area (e.g. drilling a large number of holes for the small tubes), and not considering either the flow path contraction due to by fouling or the minimum tube diameter for mechanical cleaning. The impact of cost function can be seen by comparing the FOB costs obtained through the Hall method (equation (2), denoted as $C_{FOB,H}$ in the table) and the Caputo method adaptation introduced in [24] ($C_{FOB,C}$). For Case 2A a configuration was found that is clearly cheaper in terms of $C_{FOB,H}$ than the solutions of 2B and 2C, but little or no better in terms of $C_{FOB,C}$.

To correctly evaluate the impact of cost function and problem formulation on optimization performance, the tuning of the GA was also evaluated. The MATLAB GA has several tuning parameters; exhaustive testing of all combinations of these was considered infeasible. Those for which a good estimate was considered possible, or whose impact was estimated to be comparatively small, were set at fixed values. On these grounds, the population size (number of parents, NP) was set at NP=10D, elite count N_E=0.05NP, and shrink parameter S=1.0.

Table 6. Optimum designs of different formulations of the cases.

	1A	1B	1C	2A	2B	2C
L_{tot} [m]	5.95	7.441	8.163	7.679	8.669	8.034
D_{tot} [m]	0.850	0.656	0.646	0.495	0.684	0.717
$L_{tb,tot}$ [m]	4.815	6.562	7.315	7.189	7.986	7.315
D_{sh} [m]	0.652	0.530	0.540	0.422	0.582	0.615
D_{OTL} [m]	0.638	0.517	0.507	0.334	0.492	0.524
N_{tp} [-]	1	1	1	1	4	4
θ_{tp} [°]	60	60	60	30	45	45
Tube fluid	Cold	Cold	Cold	Hot	Cold	Cold
d_o [mm]	15.88	15.88	15.88	9.52	25.4	22.2
P_T/d_o [-]	1.256	1.250	1.275	1.845	1.256	1.293
S_{bf}/D_{sh} [-]	0.910	0.936	0.991	1.000	0.500	0.487
N_{SS} [-]	7	0	0	7	2	2
N_{bf} [-]	6	11	13	15	25	23
N_{tb} [-]	860	556	510	282	128	188
w_{tb} [m/s]	0.65	1.00	1.09	0.76	1.54	1.43
BC [%]	0.20	0.25	0.31	0.24	0.20	0.29
U [W/m^{2}K]	710	800.0	782	286	238	203
Δp_{tb} [kPa]	3.0	10.0	13.0	11.2	71.6	71.0
Δp_{sh} [kPa]	10.4	27.2	24.5	6.1	0.7	0.5
C_{tot} [USD,€]	7535 *	19072	19513	3335 *	15440	15675
$C_{FOB,H}$ [USD,€]	12472 *	11370	11551	5638 *	6732	7421
$C_{FOB,C}$ [USD,€]	41156 *	31037	31573	25516 *	24673	25653

* [C] = 1982 USD

The mutation scale parameter MS, and crossover fraction CF, on the other hand, have a considerable impact on the main search mechanisms, crossover and mutation. It was deemed plausible that depending on the objective function topology, one or the other mechanism may be superior, or may need implementation in different scale or scope. These two parameters were thus investigated in more detail. The allowed value ranges were divided in a 10×10 grid, and GA run at 10 random pairs of parameters in each square. Termination criteria were finding a C_{tot} within 0.2% of those of Table 6 (success), or reaching an NFE value of 5000D on a D-dimensional case (fail). Figure 2 shows the results by circles representing a success; in squares with 10/10 successes, these are filled. Figure 3 shows the convergence speed as a surface plot of mean NFE at termination.

It is clear from the results that the discretely formulated case with a more detailed cost correlation was the hardest; success rate for both Case 1 and 2 was negligibly low. Rather than failing to converge within the allowed NFE, the GA tended to converge to local optima. In addition to being clearly multi-modal, the case is also highly non-separable; some variables have narrow feasible ranges moving over a wide range based on other variables. This requires a rotationally invariant search, which the main operator of GA, crossover, is not.

As the discrete case with a detailed cost function is also the arguably most realistic one, it was investigated further to see if it could be made easier for GA by reformulating it via a different choice of decision variables. The multimodality is an inherent, unchangeable characteristic of the problem, but reducing the degree of non-separability would assist the crossover operations in GA; this became therefore the focus of improvement attempts.

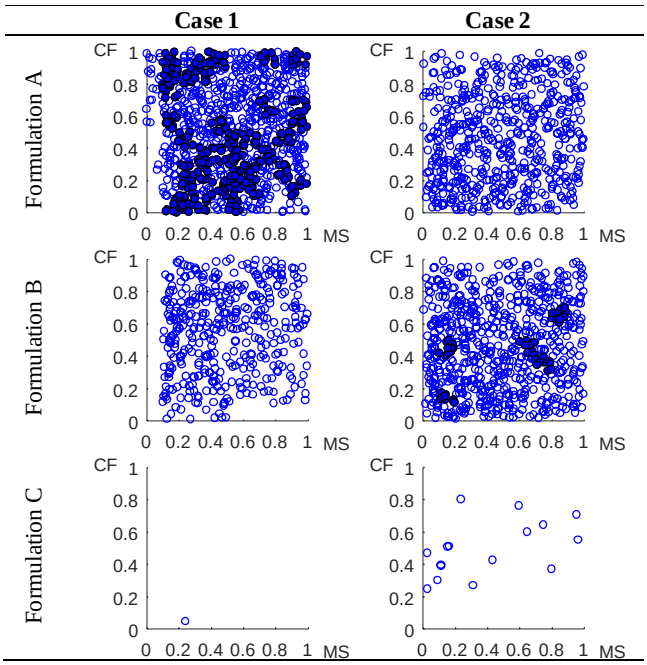

Figure 2 Successful runs with different parameter settings

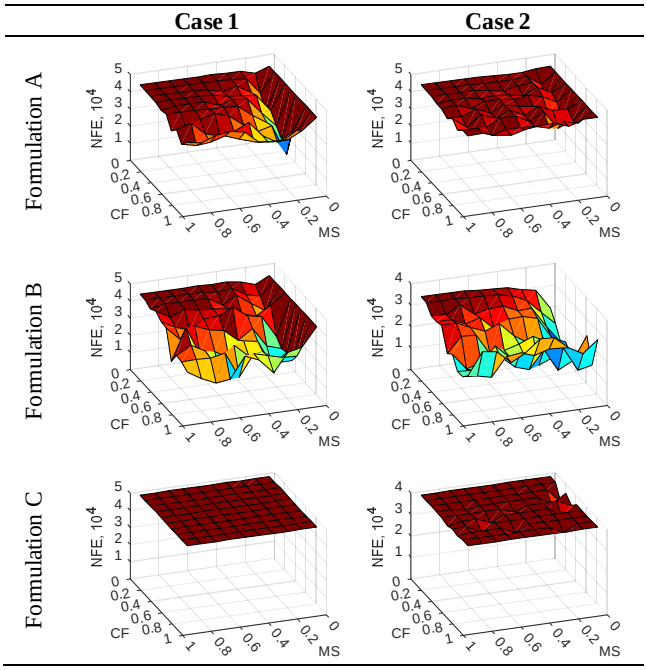

Figure 3 Average NFE with different parameter settings

The formulation was adjusted by changing variables defining the STHE geometry to ones defining, or at least more closely related to, the flows. Flow-related parameters such as velocity are likely to have good values at broadly similar magnitudes even if other values change, whereas the optimum of for example tubes per pass varies greatly depending on the tube diameter. Some objective function noise was accepted as a drawback of this, as continuous decision variables must be adjusted to become compatible with available shell diameters or tube lengths. Table 7 lists the decision variables of the new cases.

Table 7. Different formulations of the discrete Case C.

	C_0	C_1	C_2	C_3
Common variables	θ_{tp} [°], N_{tp} [-], FA [-], d_o [m], L_{tb}, [m], N_{SS} [-]			
Shell diameter; tube count & arrangement	D_{sh} [-] $N_{tb/p}$ [-]	D_{sh} [m] P/d_o [-]	w_{tb} [m/s] P/d_o [-]	w_{tb} [m/s] P/d_o [-]
Baffle cut	BC [-]	ΔBC [-], $-0.05<\Delta BC<0.05$	BC [-]	A_{wnd}/A_{crf} [-], $0.075<A_{wnd}/A_{crf}<1$
Number of baffles	N_{bfl} [-]	N_{bfl} [-]	S_{bf}/D_{sh} [-]	S_{bf}/D_{sh} [-]

Formulation C_1 implements changes that are possible without significantly rounding any value: tube count per pass is determined from tube pitch ratio and shell diameter, and baffle cut BC was changed to a deviation of actual BC from that obtained from a correlation based on a graph from [32]; actual BC is then obtained from

$$BC = 0.2 + \left(\frac{S_{bf}}{D_{sh}} - 0.2\right) \cdot \frac{0.15}{0.80} + \Delta BC. \qquad (6)$$

Problem formulations C_2 and C_3 were changed more to improve separability. In these, the tube count per pass and shell diameter are defined by tube-side velocity w_{tb} and pitch ratio P/d_o. The next higher available shell diameter is selected, and P/d_o increased to match this diameter with the given w_{tb}. The number of baffles N_{bf} is defined by the ratio of baffle spacing and shell diameter, rounded to integer, and used to determine the actual S_{bf}/D_{sh}. Formulation C_3 also defines the baffle cut as a ratio of baffle window area A_{wnd} to the widest cross-flow area A_{crf} between two baffles at shell centreline. Figures 4 and 5 show the success rate and number of function evaluations required to find the optimum. NFE_{max} was again 5000D. It is clear that the formulations C_2 and C_3, and to a lesser extent C_1, made the problem easier despite the objective function noise introduced.

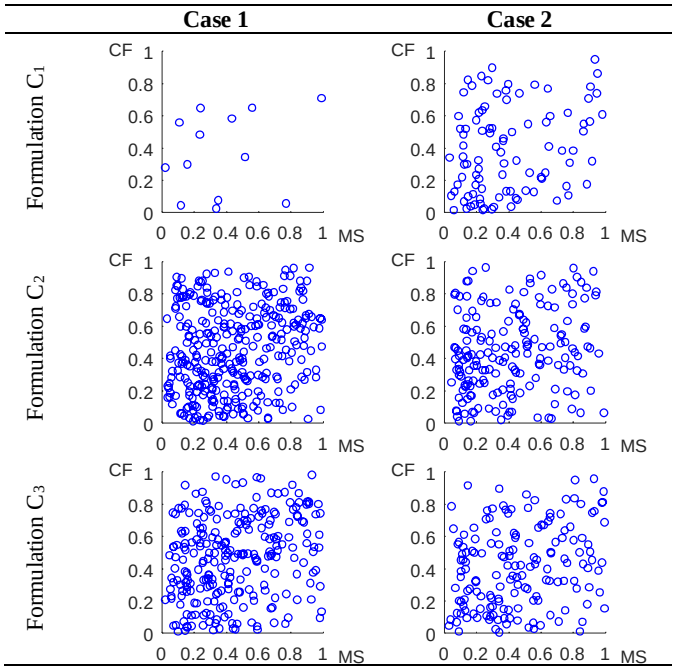

Figure 4 Successful runs with different parameter settings

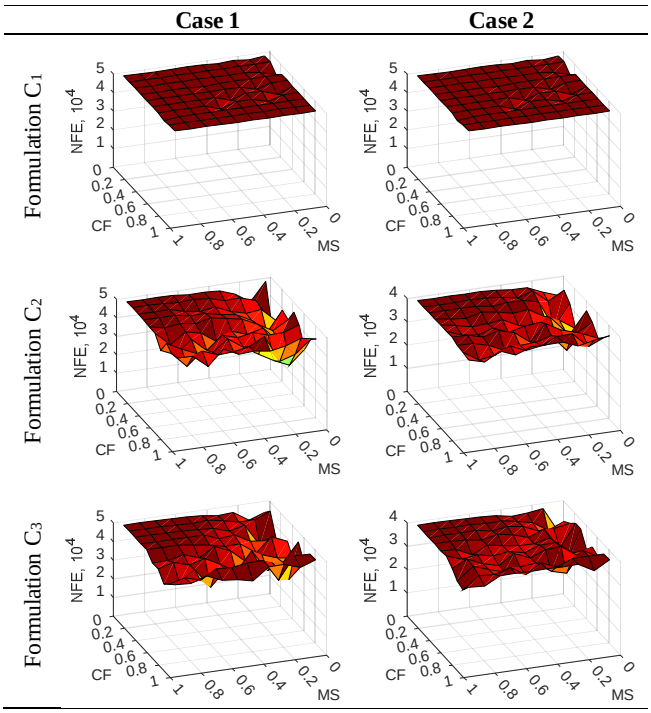

Figure 5 Average NFE with different parameter settings

CONCLUSIONS

The impact of objective function formulation and control parameter tuning on the shell-and-tube heat exchanger optimization was studied. Although STHE optimization is currently an active research topic, the selection of decision variables, cost function, and optimizer control parameter settings have received little attention. The results of this study show that these are in fact important factors that may have considerable effect on both the heat exchanger design found in the optimization, and the speed and robustness of the process.

A simple area-based correlation for heat exchanger cost was confirmed to have serious shortcomings in optimization. Such cost functions resulted in unrealistic designs by allowing performance improvement by design choices whose costs are ignored by the cost model, as suggested by Caputo et al. [21]. A simple area-based cost correlation also resulted in different optimization performance compared to the more realistic cost models. the area-based model would not be suitable to serve as substitutes for more detailed models for optimization algorithm comparisons, either. It is thus concluded that such correlations are of little value and should be avoided in STHE optimization, even though they are currently still being used in such studies.

The continuous problem formulations proved clearly easier than the discrete ones. Within the harder, but arguably more realistic discrete formulation, the importance of decision variable selection was shown. While the problem is inherently non-separable to some extent, equipment dimensions as decision variables exacerbates this. Highly non-separable problems need a rotationally invariant search, which the main mechanism of GA, crossover, is not. making GA ineffective at such problems.

Reformulation by selecting different decision variables to reduce the significant non-separability clearly improved the success rate of GA. The new formulations, however, required adjusting some decision variable values in objective function evaluation to enforce the use of standard dimensions. This made the function somewhat noisy, as some assigned variable values were only approximately, but not precisely, those of the final design. The improved separability still improved performance enough that the GA could be considered effective at the discrete case with the right formulation: reliability, while not 100 %, was sufficient that with a number of runs at $MS \approx 0.15$, the probability of finding a design very close to optimum would be high.

APPENDIX A. HEAT EXCHANGER MODEL

The heat transfer surface area (tube outside area A_o) is determined by using the ε-*NTU* method, where *NTU* is

$$NTU = \frac{U A_o}{\dot{m}_{min} c_{p,min}}. \quad (A.1)$$

The overall heat transfer coefficient U is found from

$$U = \left[\frac{d_o}{d_i}\left(R''_{tf,i} + \frac{1}{h_i}\right) + R''_w + R''_{tf,o} + \frac{1}{h_o}\right]^{-1}. \quad (A.2)$$

The tube heat transfer coefficient is obtained from the Petukhov-Popov correlation originally published in [33] as cited in [34]:

$$Nu_i = \frac{h_i d_i}{k_{f,i}} = \frac{0.125 f\, Re\, Pr}{1.07 + \frac{900}{Re} + \frac{0.65}{1+10Pr} + 12.7\sqrt{0.5 f}\, Pr^{2/3} - 1} \quad (A.3)$$

The friction factor f is obtained from the iterative Colebrook-White equation originally published in [35] as cited in [34]:

$$\frac{1}{\sqrt{f}} = -2\log_{10}\left[\frac{2.51}{Re\sqrt{f}} + \frac{K/d_i}{3.71}\right], \quad (A.4)$$

where K is the absolute surface roughness.The shell-side heat transfer coefficient is determined using the Bell-Delaware methodology for flow geometry correction factors with the Gnielinski-Gaddis heat transfer correlations as described in [36]. The shell-side heat transfer coefficient h_o is calculated from

$$Nu_o = \frac{h_o d_o}{k_{f,o}} = f_G f_L f_B f_N f_P f_A\left(0.3 + \sqrt{Nu_{lam}^2 + Nu_{turb}^2}\right), \quad (A.5)$$

where the correction factors f are for baffled shell-side flow deviation from cross-flow tube bundle (f_G), leakages through baffle-shell and baffle-tube gaps (f_L), bypass flow between tube bundle and shell (f_B), number of tubes in cross flow (f_N), fluid property variation (f_P) and tube arrangement (f_A). The equations for obtaining these are listed in reference [36]. The *Nu* for laminar and turbulent flow regimes are obtained from

$$Nu_{lam} = 0.664\sqrt{Re_{\psi,1}}\sqrt[3]{Pr} \quad (A.6a)$$

$$Nu_{turb} = \frac{0.037 Re_{\psi,1}^{0.8} Pr}{1 + 2.443 Re_{\psi,1}^{-1}\left(Pr^{2/3} - 1\right)}. \quad (A.6b)$$

The Reynolds number $Re_{\psi,1}$ is defined as

$$Re_{\psi,1} = \frac{w\, l\, \rho}{\psi \mu} \quad (A.7)$$

where w is theoretical velocity in cross-flow across shell centre-line between two baffles without tubes, $l = ½\pi d_o$, ρ is the density, μ the dynamic viscosity, and ψ is a void fraction as defined in [36]. The tube-side Δp_i is calculated from

$$\Delta p_i = \frac{\rho_i w_i^2}{2}\left(\frac{f L_{tb}}{d_i} + K_{nzl,in} + N_{tp}\left(K_{i,in} + K_{i,out}\right) + K_{nzl,out}\right) \quad (A.8)$$

where $K_{nzl,in}$ and $K_{nzl,out}$ are the loss coefficients for tube-side nozzles, and $K_{i,in}$ and $K_{i,out}$ the loss coefficients for flows in and out from the tubes. The shell-side pressure drop Δp_o is the sum of Δp in cross-flow between baffles Δp_Q, entry and exit cross flow sections Δp_{QE}, baffle windows Δp_W, and at the nozzles Δp_{nzl}:

$$\Delta p_o = (N_{bf} - 1)\Delta p_Q + 2\Delta p_{QE} + N_{bf}\Delta p_w + \Delta p_{nzl} \qquad (A.9)$$

where N_{bf} is the number of baffles. The calculation process for each pressure drop component is described in [37].

REFERENCES

[1] Asadi M., Song Y., Sunden B., and Xie G. Economic optimization design of shell-and-tube heat exchangers by a cuckoo-search-algorithm. *Appl Therm Eng* 2014, Vol 73, pp. 1032-1040

[2] Azad A.V., and Amidpour M. Economic optimization of shell and tube heat exchanger based on constructal theory. *Energy*, Vol 36, 2011, pp. 1087-1096

[3] Caputo A.C., Pelagagge P.M., and Salini P. Heat exchanger design based on economic optimisation. *Appl Therm Eng*, Vol 28, 2008, pp. 1151-1159

[4] Hajabdollahi H., Ahmadi P., Dincer I. Thermoeconomic optimization of a shell and tube condenser using both genetic algorithm and particle swarm. *Int J Refrig*, Vol34, 2011,pp.1066-1076

[5] Jegede F., Polley G. Optimum heat exchanger design: Process design, *Chem Eng Res Des*, Vol 70, 1992, pp.133-141

[6] Mizutani F.T., Pessoa F.L., Queiroz E.M., Hauan S., Grossmann I.E. Mathematical programming model for heat-exchanger network synthesis including detailed heat-exchanger designs. 1. Shell-and-tube heat-exchanger design, *Ind Eng Chem Res*, Vol 42, 2003, pp. 4009-4018

[7] Muralikrishna K., Shenoy U. Heat exchanger design targets for minimum area and cost. *Chem Eng Res Des*, Vol 78, 2000, pp.161-167

[8] Ponce-Ortega J.M., Serna-González M., Jiménez-Gutiérrez A. Use of genetic algorithms for the optimal design of shell-and-tube heat exchangers, *Appl Therm Eng*, Vol 29, 2009, pp. 203-209

[9] Babu B., Munawar S. Differential evolution strategies for optimal design of shell-and-tube heat exchangers. *Chem Eng Sci*, Vol 62, 2007, pp. 3720-3739

[10] Chaudhuri PD, Diwekar UM, Logsdon JS. An automated approach for the optimal design of heat exchangers. *Ind Eng Chem Res*, Vol 36, 1997, pp. 3685-3693

[11] Costa A.L. and Queiroz E.M. Design optimization of shell-and-tube heat exchangers, *Appl Therm Eng*, Vol 28, 2008, pp. 1798-1805

[12] Khosravi R., Khosravi A., Nahavandi S., Hajabdollahi H., Effectiveness of evolutionary algorithms for optimization of heat exchangers, *Energ Convers Manag*, Vol 89, 2015, pp. 281-288

[13] Guo J., Cheng L., Xu M. Optimization design of shell-and-tube heat exchanger by entropy generation minimization and genetic algorithm. *Appl Therm Eng*, Vol 29, 2009, pp. 2954-2960

[14] Amini M., Bazargan M. Two objective optimization in shell-and-tube heat exchangers using genetic algorithm. *Appl Therm Eng* Vol 69, 2014, pp. 278-285

[15] Daróczy L., Janiga G., Thévenin D. Systematic analysis of the heat exchanger arrangement problem using multi-objective genetic optimization. *Energy*, Vol 65, 2014, pp. 364-373.

[16] Fettaka S., Thibault J., Gupta Y. Design of shell-and-tube heat exchangers using multiobjective optimization, *Int J Heat Mass Transfer* Vol 60, 2013, pp. 343-354

[17] Sanaye S., Hajabdollahi H. Multi-objective optimization of shell and tube heat exchangers, *Appl Therm Eng*, Vol 30, 2010, pp. 1937-1945

[18] Serna M., Jiménez A. A compact formulation of the Bell–Delaware method for heat exchanger design and optimization. *Chem Eng Res Des*, Vol 83, 2005, pp. 539-550.

[19] Sadeghzadeh H., Ehyaei M., Rosen M. Techno-economic optimization of a shell and tube heat exchanger by genetic and particle swarm algorithms. *Energ Convers Manage*, Vol 93, 2015, pp. 84-91

[20] Fesanghary M., Damangir E., Soleimani I. Design optimization of shell and tube heat exchangers using global sensitivity analysis and harmony search algorithm, *Appl Therm Eng*, Vol 29, 2009, pp. 1026-1031

[21] Caputo A.C., Pelagagge P.M., and Salini P. Manufacturing cost model for heat exchangers optimization, *Appl Therm Eng*, Vol 94, 2016, pp. 513-533

[22] Hall R.S., Matley J., McNaughton K. Current Costs of Process Equipment. *Chem Eng*, Vol 89, 1982, pp. 80-83

[23] Sinnott R.K. *Coulson & Richardson's Chemical Engineering Design*, 4th ed., Vol 6., Butterworth-Heinemann, UK, 2005

[24] Saari J., Machado de Oliveira Carvalho M., Sermyagina E., Vakkilainen E., Kaikko J. Optimization of a shell-and-tube district heat condenser for a small back pressure CHP plant. *Proceedings of the 12th International Conference on Heat Transfer, Fluid Mechanics, and Thermodynamics*, Malaga, Spain, July 2016, pp. 270-277

[25] Saari J., Afanasyeva S., Vakkilainen E., Kaikko J. Heat Transfer Model and Optimization of a Shell-And-Tube District Heat Condenser. *Proceedings of the 27th International Conference on Efficiency, Cost, Optimization, Simulation and Environmental Impact of Energy Systems (ECOS)*, Turku, Finland, 2014, pp. 1920-1933

[26] Müller-Steinhagen H. Fouling of Heat Exchanger Surfaces. In: *VDI Heat Atlas*, 2nd ed., Springer-Verlag Berlin Heidelberg, 2010, pp.79

[27] Diaz-Bejarano E., Coletti F., Macchietto S. Impact of crude oil fouling composition on the thermohydraulic performance of refinery heat exchangers. *Proceedings of the 11th International Conference on Heat Transfer, Fluid Mechanics and Thermodynamics*, South Africa, 2015, pp. 600-605

[28] MathWorks. Genetic Algorithm, http://www.mathworks.com/discovery/genetic-algorithm.html. [accessed Oct 12th 2017]

[29] Patel V.K., Rao R.V. Design optimization of shell-and-tube heat exchanger using particle swarm optimization technique. *Appl Therm Eng*, Vol 30, 2010, pp. 1417-1425

[30] Hadidi A., Hadidi M., Nazari A. A new design approach for shell-and-tube heat exchangers using imperialist competitive algorithm (ICA) from economic point of view. *Energy Convers Manag*, Vol 67, 2013, pp. 66-74

[31] Hadidi A., Nazari A. Design and economic optimization of shell-and-tube heat exchangers using biogeography-based (BBO) algorithm. *Appl Therm Eng*, Vol 51, 2013, pp. 1263-1272

[32] Taborek J. Practices of shell-and-tube heat exchanger design, chapter 3.3.4. *Heat Exchangers Design Handbook 3*, Hemisphere Publishing Corporation, New York, USA, 1983

[33] Pethukov B., Popov V. Theoretical calculation of heat exchange in turbulent flow in tubes of an incompressible fluid with variable physical properties. *High Temp*, Vol 1, 1963, pp. 69-83

[34] Shah R.K., Sekulic D.P. *Fundamentals of Heat Exchanger Design*. John Wiley & Sons, New Jersey, USA, 2003

[35] Colebrook C., White C. Experiments with fluid friction in roughened pipes. *Proceedings of the Royal Society of London, Series a, mathematical and physical sciences*, 1937, pp. 367-381

[36] Gaddis E.S., Gnielinski V. Shell-Side Heat Transfer in Baffled Shell-and-Tube Heat Exchangers. In: *VDI Heat Atlas*, 2nd ed., Springer-Verlag Berlin Heidelberg, 2010, pp. 731

[37] Gaddis E.S. Pressure Drop in the Outer Shell of Heat Exchangers. In: *VDI Heat Atlas*, 2nd ed., Springer-Verlag Berlin Heidelberg, 2010, pp. 1092